Check for updates

Synthesis of polyaniline-coated composite anion exchange membranes based on polyacrylonitrile for the separation of tartaric acid *via* electrodialysis

Khurram,[a] Abdul Ghaffar, [iD] *[b] Sonia Zulfiqar, [iD] [cde] Muzzamil Khan,[b] Muhammad Latif [iD] [f] and Eric W. Cochran [iD] *[d]

The increasing need to tackle major societal challenges such as environmental sustainability and resource scarcity has heightened global interest in green and efficient separation technologies. The separation of organic acids, particularly tartaric acid, holds significant industrial importance in the food and pharmaceutical sectors. Purifying tartaric acid is crucial due to its roles as a chiral catalyst, antioxidant, and stabilizer, which are vital for ensuring product quality and efficiency. In this study, we synthesized heterogeneous anion exchange membranes by casting a solution of polyacrylonitrile (PAN) homogeneously dispersed with micronized anion exchange resin [polystyrene-divinylbenzene-trimethyl ammonium chloride (PS-DVB-TAC)]. These membranes were further coated with polyaniline (PANI) through *in situ* polymerization at different time intervals such as 2, 12, and 24 h. Cation exchange membranes were also prepared by solution casting of PAN dispersed with micronized cation exchange resin, sulfonated poly-styrene-*co*-divinylbenzene, and SPS-DVB. These synthesized anion exchange membranes with and without a PANI coating were examined for their separation performance of tartaric acid, along with the cation exchange membranes in a four-compartment electrodialyser at a constant voltage. The newly fabricated membranes were characterized by different techniques, including attenuated total reflectance-Fourier transform infrared spectroscopy for functional group analysis, scanning electron microscopy for their surface morphology, and the four-probe method for electrical conductivity. In addition, ion exchange capacity and water uptake have been measured. The electrodialysis experiments showed that 14.82 wt% of tartrate ions moved into the product compartment through the uncoated anion exchange membrane within 30 min at a voltage of 30 V. Under the same conditions, membranes coated with PANI at 2, 12, and 24 h raised the separation efficiency to 21.19%, 34.13%, and 37.21%, respectively. Findings indicate that membranes coated with PANI for extended periods demonstrate superior separation efficiency for tartaric acid. Consequently, this energy-efficient method shows significant potential for application in the food and pharmaceutical industries for separating tartaric acid and other organic and amino acids. This research can advance practical and sustainable separation technologies, addressing critical societal issues like resource efficiency and environmental sustainability.

1. Introduction

Currently, membrane separation is the most state-of-the-art and important technology among all types of separation methods

[a]Department of Chemistry, Government Graduate College Ravi Road Shahdara, Lahore-54950, Pakistan

[b]DIC Pakistan Limited, Shahrah-e-Roomi, P. O Amer Sidhu, Lahore-54760, Pakistan. E-mail: abdul.ghaffar@dic.com.pk

[c]Department of Physical Sciences, Lander University, 320 Stanley Ave, Greenwood, South Carolina 29649, USA

[d]Department of Chemical and Biological Engineering, Iowa State University, Sweeney Hall, 618 Bissell Road, Ames, Iowa 50011, USA. E-mail: ecochran@iastate.edu

[e]Department of Chemistry, Faculty of Science, University of Ostrava, 30. Dubna 22, Ostrava 701 03, Czech Republic

[f]Department of Biochemistry and Molecular Medicine, College of Medicine, Taibah University, Madinah, Kingdom of Saudi Arabia

because of its intrinsic features, such as high permeability and selectivity for the transportation of particular constituents, ease of operation, and positive impact on the environment.[1] This holds a key role in various commercial fields such as wastewater treatment,[2] petrochemical, metallurgical, bio-separation, and food.[3] Breakthrough effects on the performance of composite membranes have been reported within the realm of wastewater treatment, for instance, mitigation of fouling, better quality of permeation, and enhancement of flux.[4–11] Recent advances in membrane technology include the consideration of different types of materials for the synthesis of these membranes, along with their separation efficiency.[12–14] The materials used in the synthesis of membranes are generally composed of robust organic polymers and their derivatives. Because of their hydrophobic nature, these conventional polymers may seriously suffer from fouling, which makes them unattractive for long-lasting separation.[15–17]

Intrinsically conducting polymers (ICPs), such as PANI, conduct electricity through their conjugated polymer chains, facilitating electron conduction. Electrodialysis driven by electric fields enhances ion migration, improving ion transport efficiency across membranes.[18,19] This accelerates and optimizes tartaric acid separation from other charged species, reducing time and energy consumption and making the process sustainable and cost-effective. Moreover, ICPs offer high chemical stability and can be easily modified for specific applications, ensuring long-term functionality even under harsh conditions. Chemical modifications enhance selectivity for certain ions or molecules, improving separation efficiency for targeted compounds like tartaric acid and leading to highly effective membranes. The most commonly employed approaches used for the surface modification of membranes include surface coating, grafting, interfacial polymerization, and radiation exposure.[20–26] Recently, intrinsically conductive polymers (ICPs) with unique electrical and chemical properties have drawn attention to address the above-mentioned issues. ICPs are chemically and thermally stable conducting polymers that can combine their electrical and chemical properties to improve their separation performance. These ICPs can be employed as deposited films that can form a bond or fix firmly to the support membranes and have gained great interest as a material for membranes. Many ICPs like polythiophene (PTh), polypyrrole (PPy), and poly(3,4-ethylenedioxythiophene) (PEDOT) share attributes such as chemical stability and electrical conductivity, making them suitable for sensing and separation processes.[27] For example, PPy is notable for its easy synthesis and high conductivity, while PEDOT and PTh are valued for their flexibility, stability, and processability.[28,29] Nonetheless, these polymers often face challenges related to processability, cost, or specific application requirements. In contrast, in addition to its cost-effectiveness, and ease of synthesis at large scale, PANI is preferred for its distinctive chemical and electrical properties. PANI can be synthesized in various oxidation states, including emeraldine, leucoemeraldine, and pernigraniline, with solubility and conductivity adjustable through acid doping.[30] This versatility allows the customization of membrane properties for optimal separation performance. PANI's excellent electrical conductivity, which can be modulated *via* doping/dedoping, enhances ion transport in electrodialysis applications, leading to efficient separations.[31] Moreover, among ICPs, PANI is distinctive due to its environmental stability in both doped (conducting) and de-doped (insulating) states, alongside its acid-base chemistry. Importantly, undoped PANI is hydrophobic, while doped PANI is hydrophilic, making it suitable for separation applications.[32] In the last few decades, various membranes with PANI as a conducting material have been intensively studied.[33–42] Owing to the intractable properties of PANI, its dissolution in many solvents is difficult. The focus of various publications in previous years has been on the development of its processability, including the substitution of PANI aromatic ring with diverse types of functionalities such as $-OCH_3$, $-OH$, and a long alkyl chain or $-SO_3$, which resulted in its higher solubility in organic solvents and even in H_2O. Similarly, emeraldine (HCl salt form of PANI) shows enhanced solubility in common weakly polar organic or nonpolar solvents. Most of the base polymers are soluble in these solvents. Thus, the progress in PANI composites and blends is likely to have a serious impact on the selectivity and permeability of modified membranes.

Many studies have focused on the fabrication of solid surfaces with a thin layer of PANI coating, which subsequently acts as an active component, whereas the support material provides mechanical strength.[43,44] Various approaches to develop PANI composite membranes have been reported, such as dip coating, fractional thermal vacuum deposition, drop-casting, and electrochemical growth by galvanostatic, voltammetric, and potentiostatic methods.[45] Various studies have shown that the rate of deposition and the electronic and morphological characteristics of a thin layer of PANI depends on the nature of the substrate surface, whether it is hydrophilic or hydrophobic.[46] A substrate with a hydrophobic nature shows a more uniform deposition of PANI than a hydrophilic one. The polyacrylonitrile material used in this research is due to its thermal and mechanical stability and good hydrophobic nature.[47] In this study, polymeric membranes were synthesized using a micronized (400 mesh) anion exchange resin *via* the solution casting method by spreading on a glass plate, followed by a drying process. Anion exchange membranes with and without PANI coating were investigated for the separation efficiency of tartaric acid using an electrodialysis technique. Tartaric acid is a dicarboxylic acid commonly found in fruits such as bananas, grapes, and tamarinds. It plays a crucial role in different industries, including food, beverage, cosmetics, and pharmaceuticals.[48] In all these industries, the ability of electrodialysis to provide high purity, selective separation, and efficient operation makes it an attractive choice for various applications.[49] Electrodialysis is known for its lower energy consumption and operational simplicity, making it a more justifiable option. Electrodialysis is a superior method for the separation of tartaric acid, especially in comparison to more traditional techniques like crystallization, solvent extraction, and distillation, where a lot of energy and chemicals are required.[50–52] The uniqueness of this research is in its innovative membrane synthesis, demonstrated performance in electrodialysis, potential for industrial application, and its alignment with critical societal challenges. The study presents a novel approach to synthesizing heterogeneous anion exchange membranes by incorporating micronized anion exchange resin within a polyacrylonitrile (PAN) matrix. The additional coating of these membranes with PANI through *in situ* polymerization further distinguishes this work from existing studies. The use of PANI, a conducting polymer, in varying coating durations is particularly noteworthy, as it directly impacts the separation efficiency of tartaric acid, showcasing an innovative enhancement of membrane functionality. The research focuses on the application of these novel membranes in a four-compartment electrodialyser, specifically targeting the separation of tartaric acid. The significant improvement in separation efficiency, particularly with PANI-coated membranes, underscores the practical advantages of this approach. The detailed comparison of separation efficiencies under identical conditions provides

compelling evidence of the superiority of the PANI-coated membranes, particularly those coated for longer durations.

Additionally, its potential for sustainability and cost-effectiveness further enhances its appeal to industries seeking innovative separation technologies.[53–55] This technique has the most significant potential applications in the chemical, pharmaceutical, and food industries. This energy-efficient approach may potentially be employed for the separation of organic and amino acids in the food and pharmaceutical industries.

2. Experimental

2.1. Materials

Polystyrene-divinylbenzene-trimethyl ammonium chloride (PS-DVB-TAC) anion exchange resin and sulfonated polystyrene divinylbenzene (SPS-DVB) (mucolite PC003 ID) were obtained from the local market and used after crushing and sieving through a 400 mesh. Polyacrylonitrile (PAN) was purchased from Sigma-Aldrich, USA. Tartaric acid (99.5%) was obtained from Sigma-Aldrich, USA. Ferric chloride ($FeCl_3$), aniline, N-methyl-2-pyrrolidone (NMP), and phenolphthalein were purchased from Merck® (USA). Sodium hydroxide (NaOH) and hydrochloric acid (HCl) were purchased from Sigma-Aldrich, USA. All reagents were of analytical grade and used as received. Deionized water was used for the solution preparation during the experiments.

2.2. Characterization

Scanning electron microscopy (SEM) images were recorded using a JSM-6480LV (JEOL, Japan) microscope at different magnifications. For the determination of the particle size of anion exchange resin, a Litesizer-500 particle size analyzer (Anton Paar GmbH, Germany) with a measurement range from 0.3 nm $-$10 μm was employed. FTIR-ATR analysis was performed using an FTIR 4100 spectrophotometer (JASCO, Japan) with a 650–4000 cm^{-1} range. Electrical conductivity measurements were performed using four probe method (Keithley,

6220-Precision current source, 2182-Nanometer). A DC power supply (Adiget PS 3030DD) was used as a potential source. The mechanical testing of the membranes was performed using a Universal Testing Machine (LLOYD LS1).

2.3. Synthesis of anion exchange membranes

The anion exchange resin (PS-DVB-TAC) was ground in a grinder and immersed in deionized water for more than 24 h. After 6 h of drying at 50 °C, it was ground again with a mortar and pestle to obtain a very fine particle size (300–400 mesh). In this study, a 12 (w/w%) casting solution of PAN in N-methyl-2-pyrrolidone (NMP) was prepared by dissolving 1.2 g of PAN in 8.8 g NMP. After vigorous stirring for 4 h, it was subsequently loaded with 1.2 g anion exchange resin (50 : 50 w/w% of PAN), respectively, and stirred for another 4 h for uniform dispersion. The resin-dispersed doped solution was cast onto a glass plate using a casting blade. The coated membranes were immersed in a coagulant bath containing deionized water at 25 °C for phase inversion. The wet membranes were dried in a fume hood for 24 h at 25 °C (ambient temperature).

PANI was dip-coated onto the surfaces of the synthesized membranes. $FeCl_3$ (0.3 M) and aniline (0.4 M) solutions were separately prepared in aqueous HCl (0.4 M). Then, anion exchange membranes [PAN + (PS-DVB-TAC)] were dipped into a solution of anilinium chloride, and $FeCl_3$ solution was added dropwise to the solution for *in situ* polymerization. This PANI coating process was executed for different pieces of the same membrane for 2, 12, and 24 h. After coating, the membranes were washed with a 1 M HCl solution to remove the oligomers and then rinsed again with deionized water. Similarly, cation exchange membranes were prepared by loading the cation exchange resin (SPS-DVB) into PAN. A schematic path for the preparation of PANI-coated anion-exchange membranes is shown in Fig. 1.

Cation exchange membranes (CEM) were also prepared through solution casting, comprising PAN along with a cation exchange micronized resin [sulfonated poly(styrene-*co*-
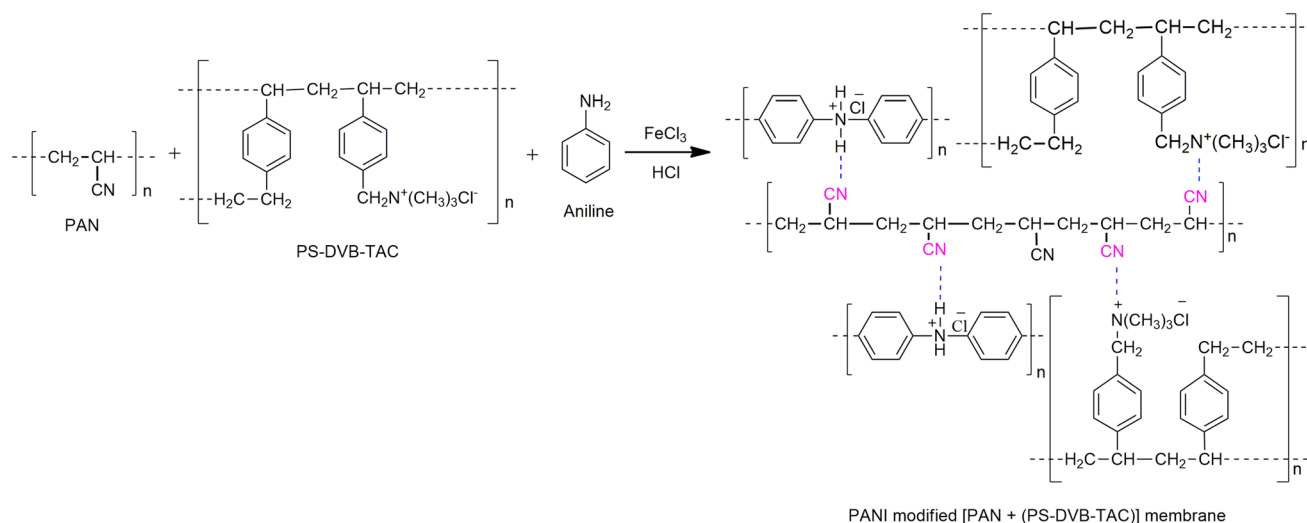

Fig. 1 Proposed route for the synthesis of the composite anion exchange membranes coated with PANI.

divinylbenzene) (SPS-DVB)] to just follow the standard procedure of electrodialysis using the method reported in the literature.[46]

2.4. Water uptake

To measure the percentage of water uptake, membranes with an area of approximately 2 cm^2 were immersed in deionized water at room temperature for 24 h for equilibration. After removing excess water with absorbent paper, the membranes were weighed, dried in an oven at 60 °C for 4 h, and subsequently weighed again. By taking the weighted difference between wet (W_{wet}) and dry (W_{dry}) membranes, the percentage of water uptake was calculated using the formula (1).[56,57]

$$\text{Water uptake}(\%) = \frac{W_{wet} - W_{dry}}{W_{dry}} \times 100 \qquad (1)$$

2.5. Assessment of ion-exchange capacity

A 2 cm^2 sample of anion exchange membrane without the PANI coating [PAN + (PS-DVB-TAC)] and PANI-coated membranes was placed separately into a 50 mL solution of 0.1 M NaOH for 24 h. The chlorides of the quaternary ammonium portion of the resin and quinoid portion of PANI were exchanged with OH$^-$ ions. The depleted OH$^-$ ions were calculated by titration using a 0.1 M HCl solution and phenolphthalein as an indicator. The membranes were then washed with deionized water and dried. The ion-exchange capacity was calculated as milliequivalents (meq g^{-1}) using the formula (2).[56]

$$\text{IEC(meq/g)} = \frac{[V_{NaOH} \times (N_1 - N_2)]}{W_{dry}} \qquad (2)$$

Where N_1 and N_2 represents the normality of NaOH before and after electrodialysis.

2.6. Electrical conductivity measurement

The electrical conductivities of the membranes with and without PANI coating were determined. In this method, 3 cm diameter membrane samples were punched using a puncher. The electrical conductivity of the membrane was measured using the four-probe method, and the distance between each probe was 0.2 cm. The membranes were very thin (140–150 μm) compared to that of the probe spacing. The electrical conductivity values were determined using the eqn (3):[58]

$$\text{Resistivity}(\rho) = \frac{V}{I} \times C \approx \left(\frac{d}{s}\right) \qquad (3)$$

Where I is the value of current and V is the voltage value obtained from the conductivity data. While C in the equation is the correction factor, its value was determined by dividing the diameter (d) of the membrane sample by the probe spacing (s). Then, the electrical conductivity was determined by taking the inverse of resistivity using the eqn (4).

$$\text{Conductivity} = \frac{1}{\text{Resistivity}} \qquad (4)$$

2.7. Electrodialysis process

The electrodialysis process was performed in an electrodialysis cell with four chambers, as shown in Fig. 2. Titanium plates were used as the cathode and the anode. The exposed area of these electrodes was 12.56 cm^2 similar to the membrane area. Self-prepared cation- and anion-exchange membranes were used for the separation of tartaric acid. A solution of Na$_2$SO$_4$ (0.1 N) was used in the cathodic and anodic chambers, and a 1% tartaric acid solution was added to the feed and product compartments separately.

Before the electrodialysis operation, the membranes were immersed in their respective solutions for 24 h. Deionized water was used to prepare all solutions. All these experiments were conducted at room temperature by applying a constant voltage of 30 V using a DC power supply for 30 min, and the separation efficiency of tartaric acid was monitored using various forms of PANI membranes by acid–base titration.[59]

3. Results and discussion

3.1. Particle size evaluation

The determination of particle size of resin in membrane technology serves to improve membrane performance by controlling pore size distribution, increasing separation efficiency, mitigating fouling, ensuring uniformity in membrane structure, and maintaining consistency in product quality across batches.[60,61] Span is a measure of the width of the particle size distribution curve and provides information on the uniformity of the particle size distribution. It was calculated using the formula (5).

$$\text{Span} = \frac{D90 - D10}{D50} \qquad (5)$$

Where, $D10$ represents the particle diameter below which 10% of the particles are present in the distribution curve, and the value for $D10$ obtained is 2.32 μm. $D50$ represents the median particle size below which 50% of the particles were found in the particle
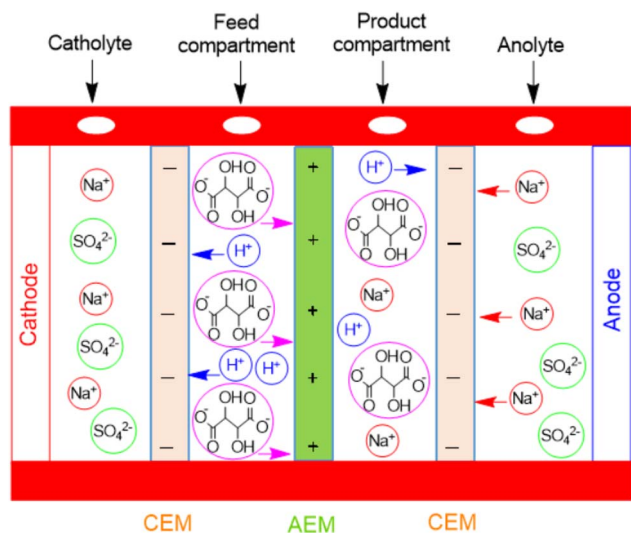

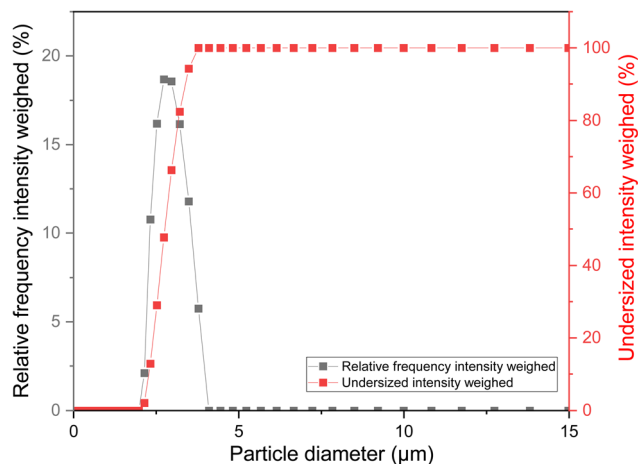Fig. 2 Experimental setup for the separation of tartaric acid using electrodialysis.

Fig. 3 Particle size determination of anionic resin (PS-DVB-TAC).

These percentiles provide a quantitative description of particle size distribution. The calculated span was 0.00039 μm. Which is closer to zero. This suggests a narrow and uniform distribution of particle sizes, which affects the morphology of the membrane. Finer resin particles resulted in a homogeneous and uniform morphology. Conversely, coarser resin particles lead to a less uniform and rougher morphology. PAN, a membrane-fabricating polymer and resin, is infusible and cannot be used to form films. Coarser resin particles hindered continuous film formation. In this study, the particle size of the resin (PS-DVB-TAC) was finely controlled to achieve a homogeneous anion exchange membrane. A larger span value represents a non-uniform and heterogeneous particle size distribution (Fig. 3).

distribution curve, and the obtained value for $D50$ was 2.83 μm. $D90$ indicates a value below which 90% of the particles occur in the distribution curve, and the value obtained for $D90$ is 3.43 μm.

3.2. Morphological analysis

The surface morphology of the membranes was evaluated through high-resolution SEM images. This helps in understanding the topography, pore structure, and any defects present on the membrane surface.[62,63] Fig. 4(a) presents an SEM image of a pure PAN membrane with a porous surface.
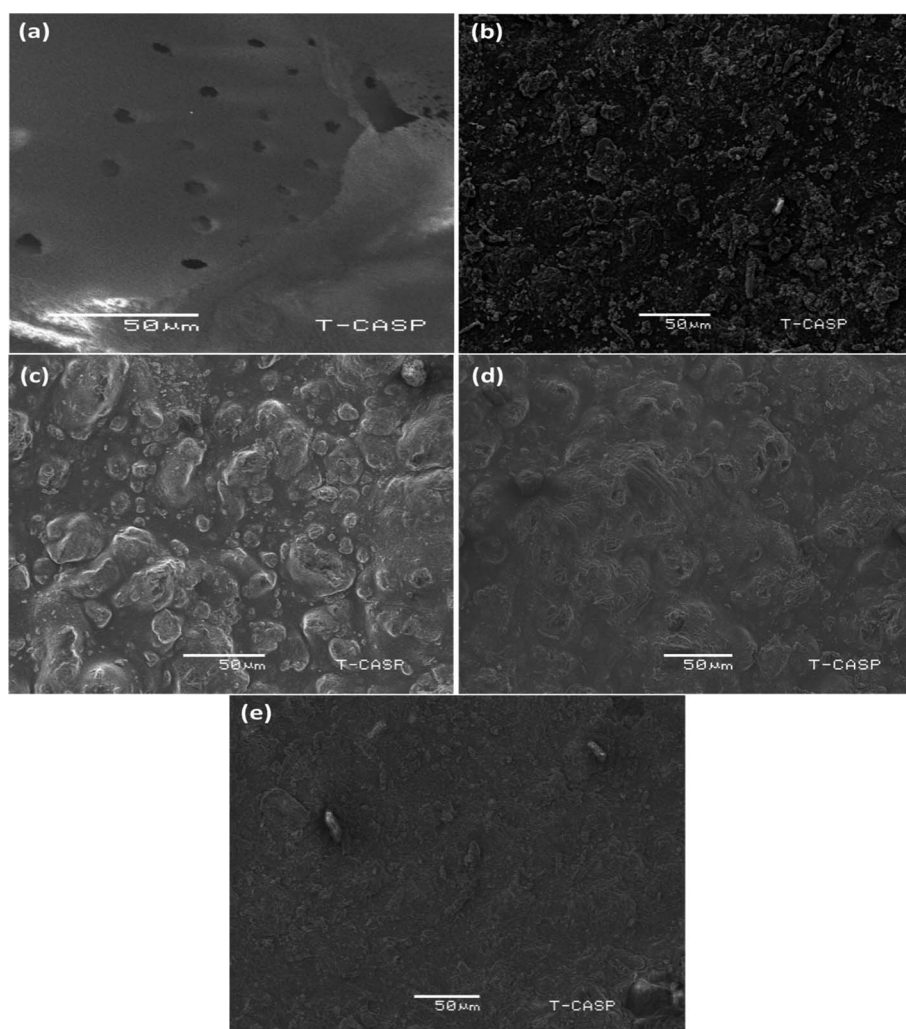

Fig. 4 SEM images of (a) pure PAN membrane (b) [PAN + (PS-DVB-TAC)], (c) [PAN + (PS-DVB-TAC)] + PANI 2 h, (d) [PAN + (PS-DVB-TAC)] + PANI 12 h, and (e) [PAN + (PS-DVB-TAC)] + PANI 24 h.
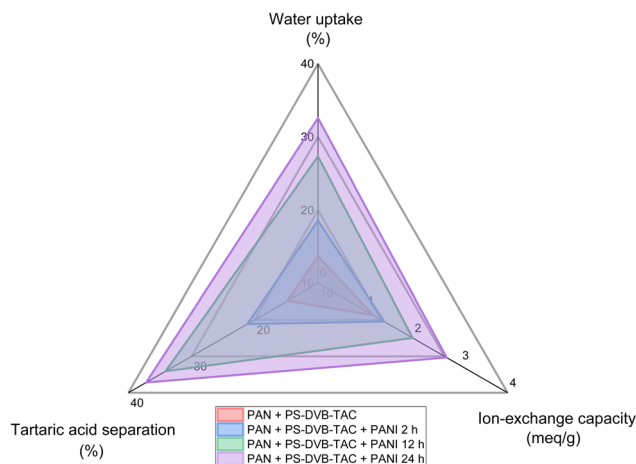
Fig. 5 Radar plot showing a comparison of different performance characteristics of the fabricated membranes.

Fig. 4(b) shows the rough texture of the surface of the membrane designed by compositing PAN with an anion exchange resin (PS-DVB-TAC). Fig. 4(c) shows the PANI coating on the surface of the composite membrane after 2 h of aniline polymerization. Fig. 4(d) presents the denser character of PANI coating of 12 h duration of aniline polymerization onto the composite membrane. Fig. 4(e) shows an even denser coating for a 24 h duration of aniline polymerization onto the composite membrane. We anticipated strong interactions between the quinoid or benzenoid part of PANI (–N = or N–H), and –CN functionalities in (PAN). Similarly, the interaction between the quaternary ammonium $[C_4(N^+)]$ component of the anion exchange resin and the functionalities of (PAN) was also evident. This might have resulted in the formation of [PAN + (PS-DVB-TAC)] with PANI.

3.3. Water uptake assessment

The percentage of water uptake in membrane technology shows membrane performance, durability, and optimization potential. It describes the understanding of transport mechanisms and intensifying energy efficiency, determining for diverse applications like desalination, biomedical engineering, and wastewater treatment.[55] The PAN membrane was hydrophobic; therefore, it did not absorb water (Fig. 5).

The water uptake of the [PAN + (PS-DVB-TAC)] membrane was (13.66 wt%) due to the quaternary ammonium functionalities of the resin in the membrane. In [PAN + (PS-DVB-TAC)] + PANI 2 h membrane, uptake of water into the membrane significantly increased (18.56 wt%) due to the collective effect of quaternary ammonium, benzenoid, and quinoid moieties. Nevertheless, in the [PAN + (PS-DVB-TAC)] + PANI 12 h membrane, the water-uptake (27.33 wt%) effectively increased with increasing duration of PANI coating. Moreover, in the [PAN + (PS-DVB-TAC)] + PANI 24 h membrane, the % age of water absorption was 32.59 wt%, which indicated that increasing the polymerization time of the PANI coating further increases its thickness. The ability of a membrane to absorb water leads to

the formation of channels or pathways, facilitating the migration of ions. As the water content increases, the diffusion path becomes more uniform and continuous, leading to more efficient ion transport across the membrane. This makes it easier for ions to travel through the membrane. The composite membrane under consideration comprises PAN, a hydrophobic polymer, dispersed with polystyrene-divinylbenzene-trimethylammonium chloride (PS-DVB-TAC), an anionic resin, and coated with ICP (PANI) for varying polymerization times. The (PS-DVB-TAC) resin contains quaternary ammonium functionality that enhances water uptake but is also crosslinked, reducing water penetration. PANI is a conducting polymer that exhibits higher hydrophilicity due to the presence of nitrogen-containing functional groups, which can form hydrogen bonds with water molecules. The modification of the anionic resin with PANI may increase the composite's overall hydrophilicity, leading to higher water uptake.[64]

A recent report indicates that a membrane with high water absorption capacity can enhance permeability, thus improving filtration or separation processes, particularly in wastewater treatment, desalination, and biomedical applications. The strong hydrophilicity associated with high water absorption reduces fouling by preventing hydrophobic interactions between the membrane surface and contaminants, thereby extending the membrane's operational life and reducing maintenance or replacement needs.[65] In drug delivery or tissue engineering, such membranes offer better-swelling properties, crucial for controlled release mechanisms or creating compatible interfaces with biological tissues.[66] For water purification, ion-exchange membranes with high water absorption can more effectively capture and exchange ions, improving pollutant removal tissues.[65] Additionally, in aqueous environments, high water absorption ensures the membrane maintains performance and structural integrity, essential for long-term effectiveness and stability.[67,68] Several investigations focus on modifying membranes with hydrophilic polymers, nanoparticles, or additional functional groups to increase water uptake and overall performance. These studies mostly employ graphene oxide, zeolites, or other hydrophilic polymers to improve membrane hydrophilicity and water flux.[69–71] The findings of our study reveal that the water uptake increases in proportion to the duration of polymerization of PANI coating. This increase can be attributed to the enhanced hydrophilicity and increased thickness of the membrane. The trend of % water uptake with increasing duration of aniline polymerization is shown in Fig. 5.

3.4. Ion-exchange capacity (IEC)

Membrane ion exchange capacity determines its ability to selectively adsorb or exchange ions, crucial for applications like water softening, desalination, and purification. It ensures efficient removal or retention of specific ions, enhancing overall separation performance.[72,73] Fig. 5 presents the ion-exchange capacity values of the [PAN + (PS-DVB-TAC)] composite membranes with and without the PANI-modified membranes. The ion exchange capacity of [PAN + (PS-DVB-TAC)] was (1.165 meq g^{-1}) which was due to the existence of exchangeable chloride

functionalities on the trimethyl quaternary ammonium. This tendency for the ion exchange capacity resembles the wt% of water uptake. The ion exchange capacity of PANI-coated membranes for 2 h increased to 1.397 meq g^{-1} because of the synergistic effect of exchangeable chloride related to quaternary ammonium (CN^+) and quinoid (–N=) functionalities. This is in good agreement with the enhanced value of water uptake for 2 h PANI-modified membrane. The IEC values for the 12 h (1.997 meq g^{-1}) and 24 h (2.714 meq g^{-1}) PANI-coated membranes further increased. This was probably due to the thicker PANI coating. A crucial feature for membranes is a high ion exchange capacity (IEC), as it significantly affects their ability to absorb and exchange ions, which is essential for applications such as desalination, water softening, and purification. A higher IEC ensures better performance by allowing for more effective removal or retention of specific ions, thereby enhancing separation efficiency and selectivity. The reported IEC values for [PAN + (PS-DVB-TAC)] membranes, which range from 1.165 to 2.714 meq g^{-1} with increasing PANI coating thickness, are notably high compared to other studies. For instance, conventional ion exchange membranes, such as Nafion, typically have IECs in the range of 0.9 to 1.1 meq g^{-1}.[74,75] In this study, higher IEC values achieved in the PANI-coated membranes are due to the increased number of ion exchange sites, particularly with thicker coatings. This suggests that the composite membranes offer superior ion exchange performance compared to other common membranes, which typically rely on a single type of ion exchange functionality. It can be inferred that by increasing the thickness of the PANI coating on the composite membrane, the number of exchangeable chlorides increased.

3.5. Structural elucidation

Fourier Transform Infrared Spectroscopy (FTIR) analysis serves to identify chemical bonds and functional groups present in a sample, aiding in material characterization, quality control,
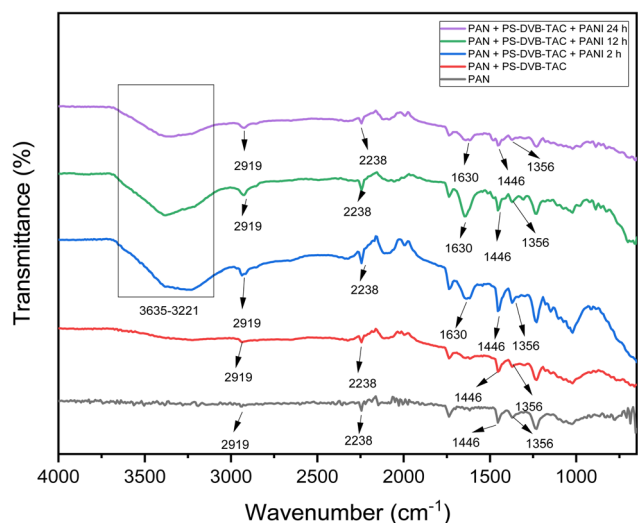

Fig. 6 FTIR-ATR spectra of pure PAN membrane, [PAN + (PS-DVB-TAC)], [PAN + (PS-DVB-TAC)] + PANI 2 h, [PAN + (PS-DVB-TAC)] + PANI 12 h, and [PAN + (PS-DVB-TAC)] + PANI 24 h.
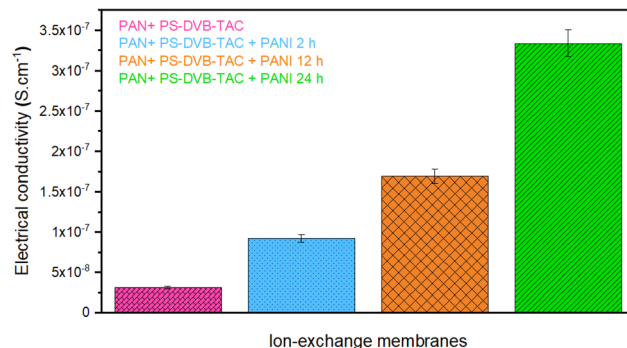

Fig. 7 Electrical conductivity of the [PAN + (PS-DVB-TAC)], [PAN + (PS-DVB-TAC)] + PANI 2 h, [PAN + (PS-DVB-TAC)] + PANI 12 h, and [PAN + (PS-DVB-TAC)] + PANI 24 h.

and understanding molecular structures in various fields like chemistry, pharmaceuticals, polymers, and environmental science.[76–78] FTIR analysis was applied to identify the functionalities present in the prepared PANI composite membranes, as presented in Fig. 6, and all the characteristic absorption bands of PAN were confirmed by their appearance in the spectra. The band at 2238 cm^{-1} confirmed the presence of the C≡N functionality;[79] however, the band at 1446 cm^{-1} was attributed to the C–H bond of CH_2 in the PAN structure.[80] The band at 1356 cm^{-1} corresponded to the quaternary ammonium (CN^+) functionality present in the anion exchange resin, and the band at 2919 cm^{-1} corresponded to the C–H stretch bond.[81] The characteristic bands of PANI appeared at 1630 cm^{-1} corresponding to C–N stretching in the quinoid and benzenoid rings.[5,82,83] The broader band at 3635–3221 cm^{-1} represents H-bonding between the C≡N group of PAN and the N–H of PANI.

3.6. Electrical conductivity measurements

The electrical conductivity of a membrane, measured *via* the four-probe method, determines its ability to conduct electricity. This is crucial for applications like fuel cells and batteries, aiding in optimizing performance, understanding charge transport mechanisms, and ensuring material integrity.[84–86] The results in Fig. 7 show that the electrical conductivity of the membrane ranged from 0.31×10^{-7} to 3.34×10^{-7} S cm^{-1}. The electrical conductivity of a PANI-modified [PAN + (PS-DVB-TAC)] composite membrane increases over time due to various structural and chemical changes that occur during the modification process. Initially, PANI is deposited onto the [PAN + (PS-DVB-TAC)] matrix. However, the PANI chains are short and may not be well-dispersed or well-interconnected. As time goes by, PANI chains grow longer and become more interconnected within the composite matrix. This leads to a higher number of charge carriers (electrons or holes) within the PANI structure, enhancing conductivity.[87] The polymer chains also become more aligned and organized, which contributes to better electron transport. Increasing the modification time allows for better dispersion of PANI throughout the [PAN + (PS-DVB-TAC)] matrix. This improved distribution means that more of the membrane's surface area is covered by conductive PANI, leading

Table 1 Mechanical properties of the different fabricated membranes

Membrane type	Tensile strength (N mm^{-2})	Stiffness (N mm^{-1})	Young's modulus (N mm^{-2})	Elongation at break (%)
PAN	1.7	0.4	23.6	10.9
[PAN + (PS-DVB-TAC)]	2.1	0.5	30.5	13.8
[PAN + (PS-DVB-TAC)] + PANI 2 h	2.0	0.8	41.6	16.9
[PAN + (PS-DVB-TAC)] + PANI 12 h	1.8	1.2	42.2	15.2
[PAN + (PS-DVB-TAC)] + PANI 24 h	1.6	2.3	44.9	14.3

Table 2 Separation efficiency of the fabricated membranes at 30 V for 30 min using electrodialysis[a]

Membrane type	A* (g/100 mL)	B* (g/100 mL)	A-B* (g)	C* (%)
[PAN +(PS-DVB-TAC)]	1.005	0.856	0.149	14.82
[PAN +(PS-DVB-TAC)] + PANI 2 h	1.005	0.792	0.213	21.19
[PAN +(PS-DVB-TAC)] + PANI 12 h	1.005	0.662	0.343	34.13
[PAN +(PS-DVB-TAC)] + PANI 24 h	1.005	0.631	0.374	37.21

[a] *Initial concentration of tartaric acid in the feed compartment (A), final conc. of tartaric acid after electrodialysis in the feed compartment (B), difference between the final and initial concentration of tartaric acid (A-B), % age separation of tartaric acid by electrodialysis (C).

to a more uniform and higher conductivity. As modification time increases, the interactions between PANI and the [PAN + (PS-DVB-TAC)] matrix improve. Better bonding at the interface can lead to more efficient charge transfer between the PANI and the surrounding matrix, further boosting the conductivity.[88] It was observed that by increasing the duration of the PANI coating, the electrical conductivity of the composite membrane increased.

3.7. Assessment of mechanical strength

The mechanical properties such as tensile strength, young modulus, stiffness, and elongation at break (%) are tabulated in Table 1. The results showed that the tensile strength of the blank PAN membrane increases with the incorporation of anion exchange resin (PS-DVB-TAC) and it is further enhanced with the deposition of PANI after 2 h. However, as the deposition time exceeds 2 h, there is a slight decline in the mechanical strength of the membranes.[89] The stiffness of the membranes increases gradually with the addition of anion exchange resin (PS-DVB-TAC) and with gradual deposition of PANI,[90] and a similar trend is observed in the case of Young's modulus. Moreover, the elongation at break (%) increases with the loading of anion exchange resin and deposition of PANI after 2 h; however, it plummets moderately as the deposition time of PANI increases.[91] This difference in mechanical results may be attributed to the presence of aromatic rings in the PANI.[92]

3.8. Electrodialysis

Electrodialysis is a membrane-based separation process widely used in various industries for desalination, water treatment, food processing, and pharmaceuticals. Its significance lies in its ability to selectively remove ions from a solution by applying an electric field across ion-selective membranes. After the process

of electrodialysis, the concentration of tartaric acid was determined in the feed chamber against 0.01 N sodium hydroxide (NaOH) using phenolphthalein as an indicator. Before electrodialysis, a blank reading was performed for 1% tartaric acid. The experimental results obtained for the separation of tartaric acid are listed in Table 2. This indicated that the composite anion exchange membrane without PANI coating can separate the tartaric acid up to 14.82 wt%. Nevertheless, the composite anion exchange membranes with PANI coating for durations of 2 h and 12 h, had 21.19 wt% and 34.13 wt% separation efficiency, respectively (Fig. 5). Moreover, the separation of tartaric acid with the 24 h PANI coating was 37.21 wt%. The findings from the modified membranes indicated that there was a rise in the percentage of tartaric acid separation as the coating of PANI increased.

4. Conclusions

Anion-exchange composite membranes were prepared by depositing a PANI coating on a heterogeneous [PAN + (PS-DVB-TAC)] membrane *via in situ* polymerization using ferric chloride as an oxidant. The SEM micrographs showed that the thickness of the PANI coating was dependent on the duration of aniline polymerization. Consequently, the PANI coating is thicker at a longer duration of polymerization of aniline compared to the shorter time. The particular interactions between the [PAN + (PS-DVB-TAC)] membrane and the PANI coating were also confirmed by FTIR analysis. The % water-uptake and ion exchange capacity are affected positively by the PANI coating; the longer the duration of PANI polymerization, the higher the % water uptake. The electrical conductivity data indicated that by increasing the PANI coating, the electrical conductivity was enhanced. The obtained results revealed that the membrane with a thicker PANI coating was more capable of separating

tartaric acid *via* electrodialysis. These membranes could potentially be implemented as energy-efficient alternatives for the separation of carboxyl-containing organic compounds from the fermentation broth and effluents of food and pharmaceutical companies.

Data availability

All data generated or analyzed during this study are included in this article.

Conflicts of interest

The authors declare that there is no conflict of interest.

Acknowledgements

References

1 M. Mulder, in *Basic Principles of Membrane Technology*, Springer, 1996, pp. 416–464.

2 A. Saravanan, P. S. Kumar, S. Jeevanantham, S. Karishma, B. Tajsabreen, P. Yaashikaa and B. Reshma, *Chemosphere*, 2021, **280**, 130595.

3 R. W. Baker, *Membrane Technology and Applications*, John Wiley & Sons, 2012.

4 B.-H. Jeong, E. M. Hoek, Y. Yan, A. Subramani, X. Huang, G. Hurwitz, A. K. Ghosh and A. Jawor, *J. Membr. Sci.*, 2007, **294**, 1–7.

5 G. L. Jadav and P. S. Singh, *J. Membr. Sci.*, 2009, **328**, 257–267.

6 A. Street, R. Sustich, J. Duncan and N. Savage, *Nanotechnology Applications for Clean Water: Solutions for Improving Water Quality*, William Andrew, 2014.

7 E. M. Hoek, M. T. M. Pendergast and A. K. Ghosh, in *Nanotechnology Applications for Clean Water*, Elsevier, 2014, pp. 133–154.

8 K. Wang, L. Xu, K. Li, L. Liu, Y. Zhang and J. Wang, *J. Membr. Sci.*, 2019, **570**, 371–379.

9 C. Li, X. Guo, X. Wang, S. Fan, Q. Zhou, H. Shao, W. Hu, C. Li, L. Tong and R. R. Kumar, *Electrochim. Acta*, 2018, **287**, 124–134.

10 R. Li, Y. Wu, L. Shen, J. Chen and H. Lin, *J. Colloid Interface Sci.*, 2018, **531**, 493–501.

11 F. Ahmed, B. S. Lalia, V. Kochkodan, N. Hilal and R. Hashaikeh, *Desalination*, 2016, **391**, 1–15.

12 K. P. Lee, T. C. Arnot and D. Mattia, *J. Membr. Sci.*, 2011, **370**, 1–22.

13 S. Nunes and K. Peinemann, *Compr. Membr. Sci. Eng.*, 2010, **2017**, 113–129.

14 M. Ulbricht, *Polym.*, 2006, **47**, 2217–2262.

15 A. Higuchi, S. Mishima and T. Nakagawa, *J. Membr. Sci.*, 1991, **57**, 175–185.

16 A. K. Ghosh and E. M. Hoek, *J. Membr. Sci.*, 2009, **336**, 140–148.

17 W. Zhang, Y. Zhu, X. Liu, D. Wang, J. Li, L. Jiang and J. Jin, *Angew. Chem., Int. Ed.*, 2014, **53**, 856–860.

18 L. Bazinet and T. R. Geoffroy, *Membr*, 2020, **10**, 221.

19 V. V. Nikonenko, N. D. Pismenskaya, E. I. Belova, P. Sistat, P. Huguet, G. Pourcelly and C. Larchet, *Adv. Colloid Interface Sci.*, 2010, **160**, 101–123.

20 H.-B. Dong, Y.-Y. Xu, Z. Yi and J.-L. Shi, *Appl. Surf. Sci.*, 2009, **255**, 8860–8866.

21 R. Patel, S. J. Im, Y. T. Ko, J. H. Kim and B. R. Min, *J. Ind. Eng. Chem.*, 2009, **15**, 299–303.

22 C. Hegde, A. M. Isloor, M. Padaki, P. Wanichapichart and Y. Liangdeng, *Desalination*, 2011, **265**, 153–158.

23 D. He, H. Susanto and M. Ulbricht, *Prog. Polym. Sci.*, 2009, **34**, 62–98.

24 W. Sun, W. Liu, Z. Wu and H. Chen, *Macromol. Rapid Commun.*, 2020, **41**, 1900430.

25 Y. Zhang, Y. Wan, G. Pan, X. Wei, Y. Li, H. Shi and Y. Liu, *J. Membr. Sci.*, 2019, **573**, 11–20.

26 D. J. Miller, D. R. Dreyer, C. W. Bielawski, D. R. Paul and B. D. Freeman, *Angew. Chem., Int. Ed.*, 2017, **56**, 4662–4711.

27 Y. Hui, C. Bian, S. Xia, J. Tong and J. Wang, *Anal. Chim. Acta*, 2018, **1022**, 1–19.

28 Z. Rahimzadeh, S. M. Naghib, Y. Zare and K. Y. Rhee, *J. Mater. Sci.*, 2020, **55**, 7575–7611.

29 M. I. Pilo, G. Sanna and N. Spano, *Chemosensors*, 2024, **12**, 81.

30 M. Gizdavic-Nikolaidis, J. M. Pupe, L. P. Silva, D. Stanisavljev, D. Svirskis and S. Swift, *Mater. Chem. Phys.*, 2022, **278**, 125676.

31 M. L. Goebel, *Evaluating the Electrical Response of Polyaniline to Mechanical Strain*, California Polytechnic State University, 2009.

32 Khurram, A. A. Qaiser, A. Ghaffar, A. Munawar, N. S. Ali and T. Hussain, *Russ. J. Electrochem.*, 2020, **56**, 587–595.

33 M. Liu, K. Tzou and R. Gregory, *Synth. Met.*, 1994, **63**, 67–71.

34 L. Rebattet, M. Escoubes, E. Genies and M. Pineri, *J. Membr. Sci.*, 1995, **57**, 1595–1604.

35 S. Bhadra, D. Khastgir, N. K. Singha and J. H. Lee, *Prog. Polym. Sci.*, 2009, **34**, 783–810.

36 L. Wen and N. Kocherginsky, *Synth. Met.*, 1999, **106**, 19–27.

37 J. Mansouri and R. Burford, *J. Membr. Sci.*, 1994, **87**, 23–34.

38 Y. Gupta, R. Wakeman and K. Hellgardt, *Desalination*, 2006, **199**, 474–476.

39 D. L. Feldheim and C. M. Elliott, *J. Membr. Sci.*, 1992, **70**, 9–15.

40 Z. Fan, Z. Wang, M. Duan, J. Wang and S. Wang, *J. Membr. Sci.*, 2008, **310**, 402–408.

41 H. Deligöz, *J. Appl. Polym. Sci.*, 2007, **105**, 2640–2645.

42 I. I. Yusoff, R. Rohani, N. Khairul Zaman, M. U. M. Junaidi, A. W. Mohammad and Z. Zainal, *Polym. Sci. Eng.*, 2019, **59**, E82–E92.

43 S. M. Hosseini, E. Jashni, M. Habibi and B. Van der Bruggen, *Ion*, 2018, **24**, 1789–1801.

44 A. Montes-Rojas, J. A. Q. Rentería, N. B. J. Chávez, J. G. Ávila-Rodríguez and B. Y. Soto, *RSC Adv.*, 2017, **7**, 25208–25219.

45 N. V. Blinova, J. Stejskal, J. M. J. Fréchet and F. Svec, *J. Polym. Sci., Part A: Polym. Chem.*, 2012, **50**, 3077–3085.

46 Khurram, A. A. Qaiser, R. Saleem, N. S. Ali, S. Nazir, T. Hussain and A. Ghaffar, *Turk. J. Chem.*, 2020, **44**, 224–236.

47 N. S. Ali, A. Ghaffar, A. A. Qaiser and M. Ahmad, *Polymer*, 2021, **45**, 68–78.

48 R. P. Walker and F. Famiani, *Hortic. Res.*, 2018, **45**, 371–430.

49 E. Kavitha, E. Poonguzhali, D. Nanditha, A. Kapoor, G. Arthanareeswaran and S. Prabhakar, *Chemosphere*, 2022, **291**, 132690.

50 A. M. Lopez and J. A. Hestekin, *Sep. Purif. Technol.*, 2013, **116**, 162–169.

51 L. Handojo, A. Wardani, D. Regina, C. Bella, M. Kresnowati and I. Wenten, *RSC Adv.*, 2019, **9**, 7854–7869.

52 J.-c. He, Y.-x. Jia, R. Yan and M. Wang, *J. Membr. Sci.*, 2021, **638**, 119683.

53 A. I. Osman, Z. Chen, A. M. Elgarahy, M. Farghali, I. M. Mohamed, A. Priya, H. B. Hawash and P. S. Yap, *Adv. Energy Sustainability Res.*, 2024, 2400011.

54 S. Arsad, A. Arsad, P. J. Ker, M. Hannan, S. G. Tang, S. Goh and T. Mahlia, *Int. J. Hydrogen Energy*, 2024, **60**, 780–801.

55 M. Sajna, T. Elmakki, K. Schipper, S. Ihm, Y. Yoo, B. Park, H. Park, H. K. Shon and D. S. Han, *Desalination*, 2023, 117065.

56 H. A. Ezzeldin, A. Apblett and G. L. Foutch, *Int. J. Polym. Sci.*, 2010, **2010**, 1–9.

57 S. Sharma, M. Dinda, C. R. Sharma and P. K. Ghosh, *J. Membr. Sci.*, 2014, **459**, 122–131.

58 F. Smits, *Bell Syst. Tech. J.*, 1958, **37**, 711–718.

59 R.-Q. Guo, B.-B. Wang, Y.-X. Jia and M. Wang, *Sep. Pur. Sci.*, 2017, **186**, 188–196.

60 P. Hillis, *Membrane Technology in Water and Wastewater Treatment*, Royal Society of Chemistry, 2000.

61 J. Mulder, *Basic Principles of Membrane Technology*, Springer Science & Business Media, 2012.

62 Z. Jia, F. Li, X. Zhang and X. Zhao, *J. Chem. Eng.*, 2023, **475**, 146287.

63 H. Isawi, *Chem. Eng. Process.*, 2023, **187**, 109343.

64 K. Dutta, S. Das and P. P. Kundu, *Polym. J.*, 2016, **48**, 301–309.

65 D. Ahmad, I. van den Boogaert, J. Miller, R. Presswell and H. Jouhara, *Energy Sources, Part A*, 2018, **40**, 2686–2725.

66 M. S. Sarwar, Q. Huang, A. Ghaffar, M. A. Abid, M. S. Zafar, Z. Khurshid and M. Latif, *Pharmaceutics*, 2020, **12**, 131.

67 P. Karami, B. Khorshidi, M. McGregor, J. T. Peichel, J. B. Soares and M. Sadrzadeh, *J. Cleaner Prod.*, 2020, **250**, 119447.

68 Y. Dong, H. Wu, F. Yang and S. Gray, *Water Res.*, 2022, **220**, 118629.

69 Y. Mao, J. Xu, H. Chen, G. Liu, Z. Liu, L. Cheng, Y. Guo, G. Liu and W. Jin, *J. Membr. Sci.*, 2023, **669**, 121324.

70 S. S. Sana, V. R. Badineni, S. K. Arla and V. K. N. Boya, *SN Appl. Sci.*, 2020, **2**, 1–10.

71 Y. Wang, H. Rong, L. Sun, P. Zhang, Y. Yang, L. Jiang, S. Wu, G. Zhu and X. Zou, *Desalination*, 2021, **504**, 114974.

72 D. Wang, Y. Zhang, H. Dong, H. Chen and A. Sengupta, *Environ. Sci.: Water Res. Technol.*, 2024, **10**, 1319–1334.

73 C. Tang and M. L. Bruening, *J. Polym. Sci.*, 2020, **58**, 2831–2856.

74 N. W. DeLuca, Nafion blend membranes for the direct methanol fuel cell, *Diss. Abstr. Int., B*, 2008, **69**, 01.

75 S. Swier, Y. S. Chun, J. Gasa, M. T. Shaw and R. Weiss, *Polym. Sci. Eng.*, 2005, **45**, 1081–1091.

76 A. Cherniienko, R. Lesyk, L. Zaprutko and A. Pawełczyk, *J. Pharm. Anal.*, 2024, **14**, 100951.

77 C.-P. S. Hsu, *Handbook of Instrumental Techniques for Analytical Chemistry*, 1997, p. 249.

78 A. Kassem, L. Abbas, O. Coutinho, S. Opara, H. Najaf, D. Kasperek, K. Pokhrel, X. Li and S. Tiquia-Arashiro, *Front. Microbiol.*, 2023, **14**, 1304081.

79 B. Mahltig, *Tekstilec*, 2021, **64**, 96–118.

80 A. Boukir, S. Fellak and P. Doumenq, *Heliyon*, 2019, **5**, e02477.

81 Y. Yu, Y. Wang, K. Lin, N. Hu, X. Zhou and S. Liu, *J. Phys. Chem. A*, 2013, **117**, 4377–4384.

82 Z. Rozlivkova, M. Trchova, M. Exnerova and J. Stejskal, *Synth. Met.*, 2011, **161**, 1122–1129.

83 Z. Morávková and E. Dmitrieva, *J. Raman Spectrosc.*, 2017, **48**, 1229–1234.

84 R.-Y. Chang, R. Li, W. Wang, W.-H. Geng, N. Li, L.-C. Jing, Z.-X. Yang, J. Li and H.-Z. Geng, *J. Membr. Sci.*, 2024, **693**, 122360.

85 M. Khan and Inamuddin, *Sci. Rep.*, 2024, **14**, 3324.

86 S. H. Yoon, H.-J. Jin, M.-C. Kook and Y. R. Pyun, *Biol. Macromol.*, 2006, **7**, 1280–1284.

87 M. Beygisangchin, S. Abdul Rashid, S. Shafie, A. R. Sadrolhosseini and H. N. Lim, *Polym.*, 2021, **13**, 2003.

88 N. Sharma, A. Singh, N. Kumar, A. Tiwari, M. Lal and S. Arya, *J. Membr. Sci.*, 2024, 1–39.

89 M. E. Uddin, R. K. Layek, N. H. Kim, D. Hui and J. H. Lee, *Composites, Part B*, 2015, **80**, 238–245.

90 I. Karbownik, O. Rac-Rumijowska, M. Fiedot-Toboła, T. Rybicki and H. Teterycz, *Mater*, 2019, **12**, 664.

91 S. S. Qavamnia and K. Nasouri, *Polym. Sci., Ser. A*, 2015, **57**, 343–349.

92 M. Jaymand, *Prog. Polym. Sci.*, 2013, **38**, 1287–1306.